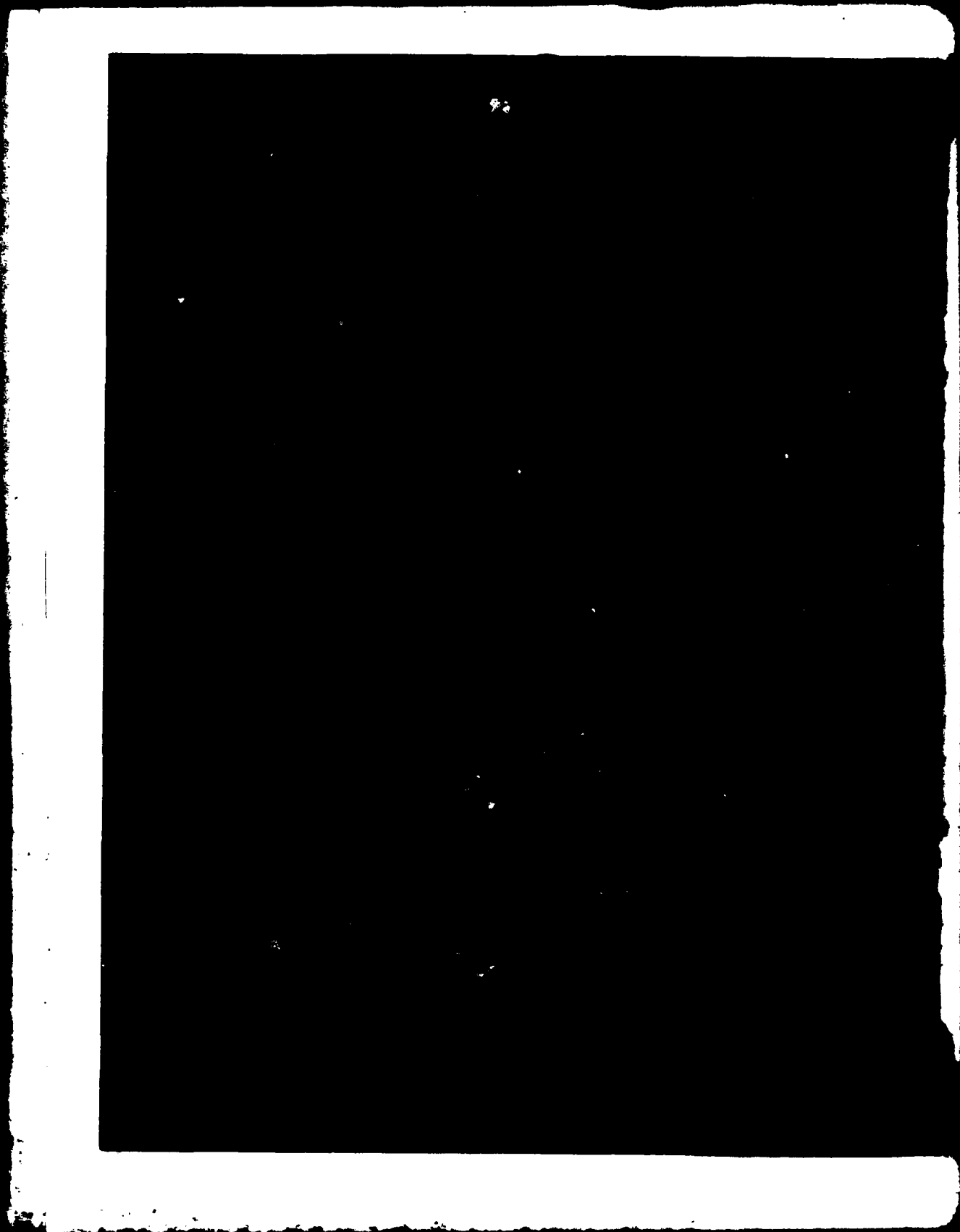


AD A099042



UNCLASSIFIED

SECURITY CLASSIFICATION OF THIS PAGE (When Data Entered)

REPORT DOCUMENTATION PAGE		READ INSTRUCTIONS BEFORE COMPLETING FORM	
1. REPORT NUMBER HDL-TR-1946	2. GOVT ACCESSION NO. AD-A099042	3. RECIPIENT'S CATALOG NUMBER	
4. TITLE (and Subtitle) Short Pulse Nd:YAG Laser for Optical Fuze Applications.		5. TYPE OF REPORT & PERIOD COVERED Technical Report	6. PERFORMING ORG. REPORT NUMBER
7. AUTHOR(s) Ronald Wellman Joseph Nemarich		8. CONTRACT OR GRANT NUMBER(s) KJ 277	
9. PERFORMING ORGANIZATION NAME AND ADDRESS Harry Diamond Laboratories 2800 Powder Mill Road Adelphi, MD 20783		10. PROGRAM ELEMENT, PROJECT, TASK AREA & WORK UNIT NUMBERS Program El.: 6.11.02.A	
11. CONTROLLING OFFICE NAME AND ADDRESS U.S. Army Materiel Development and Readiness Command Alexandria, VA 22333		12. REPORT DATE February 1981	13. NUMBER OF PAGES 35
14. MONITORING AGENCY NAME & ADDRESS (if different from Controlling Office)		15. SECURITY CLASS. (of this report) UNCLASSIFIED	
16. DISTRIBUTION STATEMENT (of this Report) Approved for public release; distribution unlimited.		15a. DECLASSIFICATION DOWNGRADING SCHEDULE	
17. DISTRIBUTION STATEMENT (of the abstract entered in Block 20, if different from Report)			
18. SUPPLEMENTARY NOTES HDL Project: A44817 DRCMS Code: 611102.H.440011 DA Project: 11.161192AH44			
19. KEY WORDS (Continue on reverse side if necessary and identify by block number) Optical fuze Nd:YAG laser Short pulse			
20. ABSTRACT (Continue on reverse side if necessary and identify by block number) The Nd:YAG laser system for potential use in optical proximity fuze systems has been investigated. The baseline source requirements are pulse width in the 10-ns range, repetition rate greater than 1 kHz, and peak power of 100 W or more. The output capabilities of four different modulation techniques have been considered. These systems include Q-switching, cavity dumping, double Q-switching, and mode locking. Both continuously pumped and flash-			

DD FORM 1 JAN 73 1473 EDITION OF 1 NOV 65 IS OBSOLETE

UNCLASSIFIED

SECURITY CLASSIFICATION OF THIS PAGE (When Data Entered)

UNCLASSIFIED

SECURITY CLASSIFICATION OF THIS PAGE(When Data Entered)

20. ABSTRACT (Cont'd)

Flashlamp pumped systems were considered, and the experimental agreement with the presented theory was good.

This investigation showed that three of the systems did not meet the baseline requirements. Q-switching was eliminated because of repetition rate limitations in the flashlamp pumped system and pulse width limitations in the continuously pumped system. Double Q-switching was eliminated for the same reasons. Mode locking was discarded because the pulse width is too narrow and the peak power is too low. The continuously pumped cavity dumped system is the only one that can meet the baseline requirements. A possible continuously pumped system using laser diodes to pump the laser rod also could meet the requirements. A careful evaluation of these systems with respect to space, power requirements, and cost would be required to determine the practicability of these systems in any particular fuze system.

Accession For	
INDEXED	X
ABSTRACTED	
FILED	
A	

UNCLASSIFIED

2 SECURITY CLASSIFICATION OF THIS PAGE(When Data Entered)

CONTENTS

	<u>Page</u>
1. INTRODUCTION.....	5
2. Q-SWITCHING.....	5
2.1 Theory.....	5
2.2 Experimental Results.....	9
3. CAVITY DUMPING.....	18
3.1 Theory.....	18
3.2 Experimental Results.....	21
4. Q-SWITCHED CAVITY DUMPING.....	21
4.1 Theory.....	21
4.2 Experimental Results.....	23
5. MODE LOCKING.....	25
6. SYSTEM CONSIDERATIONS.....	28
7. SUMMARY.....	30
LITERATURE CITED.....	31
DISTRIBUTION.....	33

FIGURES

1 Relationship between initial and final inversion levels for Q-switched operation.....	8
2 Setup for flashlamp pumped laser system operating in Q-switched mode.....	10
3 Energy output versus pump input for flashlamp pumped system to determine threshold pumping levels.....	10
4 Plot of $-\ln R_0$ versus pump threshold to determine cavity losses for data of figure 3.....	12
5 Oscilloscope photograph of shortest Q-switched pulse observed with flashlamp pumped system.....	16

FIGURES (Cont'd)

	<u>Page</u>
6 Q-switching setup for continuously pumped Nd:YAG laser rod.....	17
7 Laser output parameters versus input pump power to determine laser threshold and combined losses for continuously pumped system.....	17
8 Oscilloscope photograph of shortest Q-switched pulse obtained with continuously pumped system.....	18
9 Block diagrams of two cavity dumping techniques.....	19
10 Oscilloscope photograph of cavity dumped pulse observed by using setup of figure 9(b) and flashlamp pumped Nd:YAG rod.....	21
11 Double Q-switching setup using two kinds of Pockels cells.....	23
12 Oscilloscope photographs of double Q-switched pulse observed with 1-ns response detector and Q-switched pulse observed through 75-percent mirror using 4-ns response detector.....	24
13 Cavity mode characteristics of inhomogeneously broadened laser.....	26
14 Typical mode locking setup using mirrors, Brewster-Brewster Nd:YAG rod, and acousto-optic modulator.....	27

TABLES

1 Cavity Configuration.....	12
2 Measured and Calculated Q-Switched Pulse Parameters with $l' = 54.5$ cm and $R_o = 0.4$	13
3 Measured and Calculated Q-Switched Pulse Parameters with $l' = 54.5$ cm and $R_o = 0.6$	14
4 Measured and Calculated Q-Switched Pulse Parameters with $l' = 54.5$ cm and $R_o = 0.75$	15
5 Measured and Calculated Q-Switched Pulse Parameters with $l' = 74.5$ cm and $R_o = 0.6$	16
6 Calculated Q-Switched Pulse Widths for Continuously Pumped Laser.....	18

1. INTRODUCTION

Recent investigations of active optical proximity fuzing have largely centered upon use of pulsed gallium arsenide (GaAs) laser diodes as the source of radiation. However, for systems where relatively long range detection of targets is required, it is not always possible to obtain the high peak power and short pulses required when using laser diodes. To achieve peak powers in the 100-W to 1-kW range, laser diodes are connected in series parallel combinations. The high current required and the connecting lead inductance make it difficult to generate pulse widths less than 10 ns. Simultaneously, this configuration increases the source size, thereby increasing the transmitter divergence or beam spread. The expanded transmitter field limits the usefulness of this technique for long range fuze systems.

In this investigation, the potential of the neodymium:yttrium aluminum garnet (Nd:YAG) laser as a source for optical fuzing systems is examined. The source requirements are short pulse length, preferably in the 10-ns range; repetition rates greater than 1 kHz; and peak powers of greater than 100 W. A source of this type would apply to advanced air defense or ballistic missile systems. Other applications might be for active or semiactive optical guidance systems or optical communications links. The primary concern of this work was optical proximity fuze systems, so the Nd:YAG laser system has been evaluated from a fuzing standpoint only.

There are different ways to generate short optical pulses with an Nd:YAG laser.¹ Four methods have been examined for applications to optical fuze systems. These are (1) Q-switching, (2) cavity dumping, (3) double Q-switching, and (4) mode locking. Each of these methods has its advantages and disadvantages, and each one is detailed in the following sections. To better understand what the various modulation techniques are and how well they are explained by current theory, several were investigated here using a flashlamp pumped Nd:YAG laser. The difficulty of achieving repetition rates in the kilohertz range probably rules out this type of excitation for optical fuze application, but it proved useful for this investigation.

2. Q-SWITCHING

2.1 Theory

Operation of a laser in the Q-spoiled mode can result in an increase in its peak power and reduction in pulse width. In this

¹W. Koechner, *Solid State Laser Engineering*, Springer-Verlag New York, Inc., New York (1976).

method, an optical switch is used to keep the cavity Q low while the population inversion is built up in the laser medium. When the optical switch is turned on, the cavity Q becomes high and oscillation occurs. Since the population inversion is now much higher than the threshold inversion, the laser pulse builds up to its peak value in a very short time. This method of operation was first reported by Hellwarth in 1961.² He observed this type of operation by using a Kerr cell in the cavity of a ruby laser and achieved peak powers three orders of magnitude greater than those observed in normal pulse operation. Since these initial experiments, the theory of Q-switching has been developed in detail.³⁻⁵

An understanding of the formation of a Q-switched laser pulse follows from the laser rate equations. A particularly important parameter for efficient Q-switching is the spontaneous lifetime of the upper laser state, which is denoted by t_s . This parameter determines the length of time that the energy can be stored effectively in the laser medium. For effective Q-switching, t_s must be longer than the time required for the evolution of the giant pulse, and in fact it is beneficial to have t_s greater than the pumping time for a flashlamp pumped system. An analysis of the rate equations has been given by Wagner and Lengyel.⁵ Their results may be used to estimate the energy, the peak power, and the pulse width for an Nd:YAG laser for several different initial conditions. With a few changes in notation and with the assumption that the decay from the lower laser state to the ground state is instantaneous, their equations for peak power and energy become

$$P = \frac{h\nu \ln \left(\frac{1}{R_0} \right)}{t_R} n_t \left\{ \frac{n_i}{n_t} - \left[1 + \ln \left(\frac{n_i}{n_t} \right) \right] \right\}, \quad (1)$$

$$E = h\nu n_t \left(\frac{n_i}{n_t} - \frac{n_f}{n_t} \right) \frac{\ln \left(\frac{1}{R_0} \right)}{\ln \left(\frac{1}{R_0} \right) + L}. \quad (2)$$

²R. W. Hellwarth, *Advances in Quantum Electronics*, Columbia University Press, New York (1961), 334-341.

³F. J. McClung and R. W. Hellwarth, *Characteristics of Giant Optical Pulsations from Ruby*, *Proc. IEEE*, 51 (1963), 46-53.

⁴A. A. Vuylsteke, *Theory of Laser Regeneration Switching*, *J. Appl. Phys.*, 34 (1963), 1615-1622.

⁵W. G. Wagner and B. A. Lengyel, *Evolution of the Giant Pulse in a Laser*, *J. Appl. Phys.*, 34 (1963), 2040-2046.

Defining the half-power pulse width for a Lorentzian pulse as E/P , the pulse width is given by

$$t_p = t_c \frac{\frac{n_i}{n_t} - \frac{n_f}{n_t}}{\frac{n_i}{n_t} - \left[1 + \ln\left(\frac{n_i}{n_t}\right) \right]} \quad (3)$$

In equations (1) to (3), V is the volume of the laser medium; $h\nu$ is the photon energy; R_o is the output mirror reflectivity (the rear mirror reflectivity is assumed to be unity); t_R is the laser pulse cavity round-trip time, $2\ell'/c$; ℓ' is the effective cavity length; c is the speed of light; n_t is the threshold inversion density; n_i is the initial inversion density; n_f is the final inversion density; L is the fractional loss per round trip due to scattering, diffraction, and absorption in the cavity; and t_c is the cavity decay (fall) time. The expression for t_c is¹

$$t_c = \frac{2\ell'}{c(L - \ln R_o)} \quad (4)$$

Examining equation (3), it is apparent that the limiting value of t_p is given by t_c . Since t_c is the cavity decay time, it would appear that the rise time of the pulse would become very short for high initial inversion levels. It actually does for high initial inversion levels. But for low initial inversion levels, $n_i/n_t \approx 2$, where the pulse width can be $4t_c$ or $5t_c$, the equation implies that the rise time becomes long compared with the fall time. This effect does not occur, but is due to the approximations used to generate equation (3). An actual computer solution of the Q-switched pulse formation was done by Wagner and Lengyel.⁵ Their results show that the fall time is always longer than the rise time and that the pulse width approaches t_c for high initial inversion levels. In fact, for $n_i/n_t = 10$, the half-power pulse width is about $1.2t_c$. The pulse widths obtained by using their computer solutions agree quite well with those obtained from equation (3). However, the pulse shape that would be expected from equation (3) occurs only for high initial inversion levels, $n_i/n_t > 6$. The observed pulse shapes more closely resemble those calculated by Wagner and

¹W. Koechner, *Solid State Laser Engineering*, Springer-Verlag New York, Inc., New York (1976), 77.

⁵W. G. Wagner and B. A. Lengyel, *Evolution of the Giant Pulse in a Laser*, *J. Appl. Phys.*, 34 (1963), 2040-2046.

Lengyel, but a quick estimate of the pulse width can be obtained from equation (3). Wagner and Lengyel show also that the initial, final, and threshold inversion levels are related by the following expression:

$$\frac{n_i}{n_t} = \frac{\ln \left(\frac{n_f}{n_i} \right)}{\left(\frac{n_f}{n_i} \right) - 1} . \quad (5)$$

This expression is plotted in figure 1. By using the figure, the final inversion level or energy utilization factor can be found once the threshold and initial inversion levels are determined. The threshold inversion can be estimated from⁶

$$n_t = 8\pi n^3 t_s \Delta\nu / c t_c \lambda^2, \quad (6)$$

where n is the index of refraction of the laser medium, $\Delta\nu$ is the fluorescence line width of the laser medium, and λ is the laser wavelength. The ratio of n_i/n_t can be calculated also from the ratio of the measured initial pumping level to the measured threshold pumping level, and then n_f can be found by using equation (5) or figure 1. With

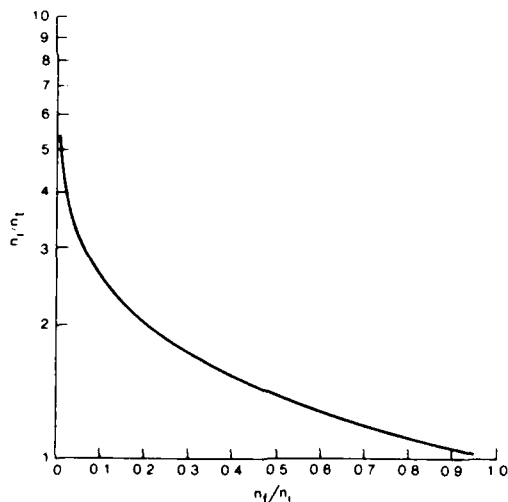


Figure 1. Relationship between initial and final inversion levels for Q-switched operation (plot of eq 5).

⁶A. Yariv, *Optical Electronics*, Holt, Rinehart & Winston, Inc., New York (1966), 165.

these values of n_t , n_i , and n_f , the pulse energy, the peak power, and the pulse width of the Q-switched pulse can be calculated. Since these values are only approximate, an experimental investigation was carried out to determine the amount of error involved in using these estimates. The theory can then be used to estimate the performance of any particular Q-switched system. The experimental results are discussed and compared with the theory in section 2.2.

2.2 Experimental Results

Q-switched sources were investigated with two types of Nd:YAG laser systems. One was a pulsed system capable of producing 50 mJ of output energy for a flashlamp input of 42 J. The repetition rate of the system is limited to 10 Hz because of the flashlamp cooling requirements and the recharging capability of the power supply. This laser was used to extend the range of investigation of Q-switching behavior. The other system was a 1-W continuous wave (cw) Nd:YAG laser that is pumped by two 1-kW tungsten halogen lamps. This system requires a relatively large water cooler to carry away the heat generated by the lamps. Current commercial cw Nd:YAG lasers are somewhat more efficient than the one used for this investigation, typical efficiencies being about 0.1 percent. This laser was investigated because it is similar to the type of laser that might apply to an optical fuze system.

The performance of the flashlamp pumped Nd:YAG laser was investigated by using the cavity configuration of figure 2. The cavity length and the output mirror reflectivity were both varied to achieve different laser thresholds and output pulse widths. The laser rod had a diameter of 0.63 cm, a length of 7.94 cm, and an active volume of 2.47 cm³. The Q-switching action was achieved with the Glan Thompson polarizer and the quarter-wave Pockels cell. When 6 kV is applied to the Pockels cell, linearly polarized light at 1.06 μ m passing through the cell is transformed to circularly polarized light. When the radiation is reflected through the Pockels cell by the output mirror, it is transformed back to linear polarization, but rotated 90 deg with respect to its original direction. This radiation is ejected from the cavity by the escape window, effectively keeping the cavity Q low while voltage is applied to the Pockels cell. When the maximum population inversion is reached in the laser rod, the voltage is removed from the Pockels cell, and it becomes inactive. The Q of the cavity is now very high. Since the population inversion is well above threshold, the Q-switched pulse is formed in a very short time.

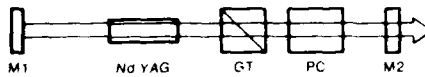


Figure 2. Setup for flashlamp pumped laser system operating in Q-switched mode: rear mirror (M1), output mirror (M2) Nd:YAG rod, Glan Thompson escape window (GT) used as polarizer, and quarter-wave Pockels cell (PC).

To measure the threshold level of the laser and to estimate the losses in the cavity, the following procedure was followed. The polarizer and the Pockels cell were placed in the cavity, but no voltage was applied to the Pockels cell. The laser was operated in the normal pulsed mode of operation with the additional cavity losses due to the polarizer and the Pockels cell. The output energy was measured as a function of pump energy; as expected, the plotted results showed a linear dependence of output energy on pump energy. By extrapolating the straight line through these points to zero output energy, the pumping threshold level was determined. This procedure was carried out for a cavity length, l , of 45.7 cm and output mirror reflectivity, R_o , of 0.4, 0.6, and 0.75 and for $l = 65.7$ cm and $R_o = 0.6$. The rear mirror reflectivity was approximately unity for all cases. The results are plotted in figure 3.

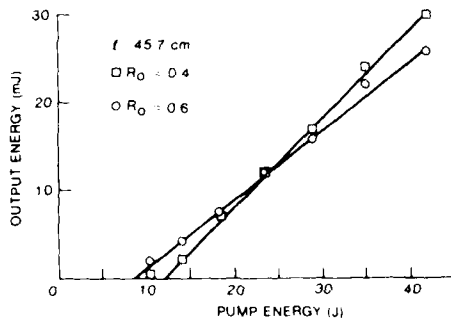
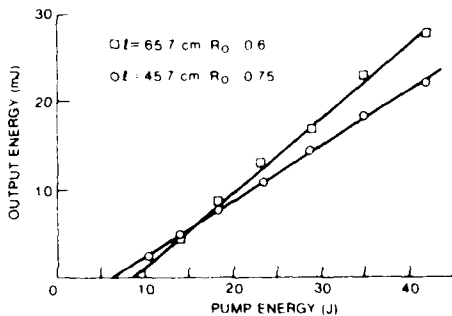


Figure 3. Energy output versus pump input for flashlamp pumped system to determine threshold pumping levels (l = cavity length and R_o = output mirror reflectivity).



To find the total loss in the cavity, $-\ln R_0$ is plotted versus the corresponding threshold pump level. The threshold pump level, the point where the total loss equals the gain, the cavity loss, and the output mirror reflectivity are related by¹

$$-\ln R_0 = 2kP_{th} - L,$$

where k is the pumping efficiency and P_{th} is the threshold pumping level. The results obtained are plotted in figure 4. Only the data for the shorter cavity are plotted in figure 4 since to find the losses more than one data point is needed. However, the total losses for the longer cavity are assumed to be the same as for the shorter cavity for all calculations. From the figure, the total cavity loss, L , is equal to 0.48. By using this value of L along with the threshold pumping levels and the physical parameters of the laser, the characteristics of the Q-switched pulse can be calculated. The relevant system parameters are

$$l' = 54.5 \text{ cm}, 74.5 \text{ cm},$$

$$R_0 = 0.4, 0.6, 0.75,$$

$$V = 2.47 \text{ cm}^3,$$

$$h\nu = 1.87 \times 10^{-12} \text{ erg},$$

$$n = 1.8,$$

$$\Delta\nu = 1.8 \times 10^{11} \text{ Hz},$$

$$t_s = 5.5 \times 10^{-4} \text{ s},$$

$$\lambda = 1.06 \times 10^{-4} \text{ cm},$$

$$L = 0.48.$$

The values of t_R , t_C , and n_t calculated from these values for each configuration are given in table 1. The value of n_t was estimated by using equation (6).

¹W. Koechner, *Solid State Laser Engineering*, Springer-Verlag New York, Inc., New York (1976), 86.

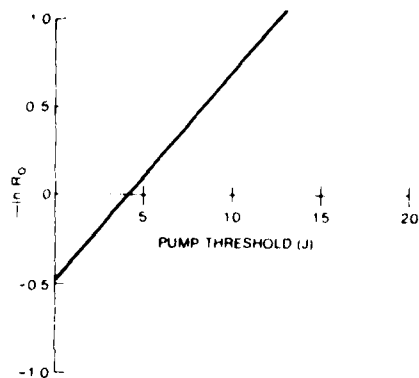


Figure 4. Plot of $-\ln R_0$ versus pump threshold to determine cavity losses for data of figure 3 for cavity length $l = 45.7$ cm only.

TABLE 1. CAVITY CONFIGURATION

Parameter	Configuration			
	A	B	C	D
Effective cavity length, l' (cm)	54.5	54.5	54.5	74.5
Output mirror reflectivity, R_0	0.4	0.6	0.75	0.6
Laser pulse cavity round-trip time, t_R (ns)	3.6	3.6	3.6	5.0
Cavity decay time, t_c (ns)	2.6	3.6	4.7	5.05
Threshold inversion density, n_t (cm^{-3})	1.65×10^{16}	1.18×10^{16}	9.16×10^{15}	8.52×10^{15}

By using these values in equations (1) to (3), the peak power, the pulse energy, and the pulse width for each cavity configuration were calculated. They are presented along with the measured values for each configuration in tables 2 to 5. In all configurations, the measured pulse widths are longer than the calculated values, and the measured peak powers are less than the calculated values. However, the measured energies are generally greater than the calculated values. Since the formulas used for estimating the pulse parameters were only approximate, the agreement between the calculated values and the measured values is good. To calculate the pulse parameters more accurately, the rate equations must be solved by computational methods. For quick estimates of pulse parameters, the approximate equations are adequate if a factor-of-two error can be tolerated. In addition, the measured pulse widths should be longer than the calculated values because of the switching

time of the Pockels cell, which was about 10 ns. This time was assumed to be zero in the derivation of equation (3). The shortest pulse was observed with the 54.5-cm cavity and an output mirror reflectivity of 0.6. The initial inversion was 4.8 times the threshold. Figure 5 shows an oscilloscope trace of the pulse as observed with a high-speed photodiode. There is some spread in the data due to flashlamp variations that produce gain variations in the laser rod. This variation in gain was discovered in making some single pass gain measurements on this particular laser rod. From tables 2 to 5, it seems that this laser system can produce 10-ns pulses with peak powers up to 1 MW. However, the repetition rate is limited to 10 Hz.

TABLE 2. MEASURED AND CALCULATED Q-SWITCHED PULSE PARAMETERS WITH $l' = 54.5$ cm AND $R_o = 0.4$

n_i/n_t	Measured			Calculated		
	P (kW)	E (mJ)	t_p (ns)	P (kW)	E (mJ)	t_p (ns)
1.1	-	-	-	9	0.7	78
1.2	210	10	50	34	1.7	49
1.55	580	23	40	220	4.8	22
1.96	580	22	38	560	7.7	14
2.4	585	18	36	1200	10.5	9
2.9	830	25	30	1700	13.5	8
3.5	835	25	30	2400	17.0	7

Notes:

l' = effective cavity length.
 R_o = output mirror reflectivity.
 n_i = initial inversion density.
 n_t = threshold inversion density.

P = peak power.
 E = peak energy.
 t_p = pulse width.

TABLE 3. MEASURED AND CALCULATED Q-SWITCHED PULSED PARAMETERS WITH $l' = 54.5$ cm
AND $R_o = 0.6$

n_i/n_t	Measured			Calculated		
	P (kW)	E (mJ)	t_p (ns)	P (kW)	E (mJ)	t_p (ns)
1.1	-	-	-	4	0.4	109
1.6	27	1	46	102	2.9	29
2.1	95	3	30	280	4.9	17
2.7	350	6	18	530	6.8	13
3.3	660	10	15	850	8.8	10
4.0	990	13	13	1200	11.0	9
4.8	1030	13	12	1700	13.0	8

Notes:

l' = effective cavity length.
 R_o = output mirror reflectivity.
 n_i = initial inversion density.
 n_t = threshold inversion density.

P = peak power.
 E = peak energy.
 t_p = pulse width.

To investigate Q-switching of a type of laser that might be useful for optical fuze applications, a 1-W cw Nd:YAG laser was set up as shown schematically in figure 6. The Q-switching action is accomplished in the same manner as the pulsed system, but the timing is not as critical since the pumping is continuous. Three different sets of mirrors were used for these experiments; the values of R_1, R_2 were 0.96, 0.92, and 0.88. The effective cavity length was 55 cm for all cases. By operating the laser continuously with all Q-switching elements in the cavity, the output power was measured for various pumping levels with each set of mirrors. Figure 7 plots these data in the same form as figures 3 and 4. The maximum pumping level is 1830 W, so the values of n_i/n_t are 1.35, 1.16, and 1.026 for the 0.96, 0.92, and 0.88 mirrors, respectively. The value of the cavity loss, L , is 0.22 from figure 7. By using equation (4) to calculate t_c and figure 1 to find the value of n_f/n_i , equation (3) can be used to calculate the pulse width. The calculated and measured values are given in table 6.

TABLE 4. MEASURED AND CALCULATED Q-SWITCHED PULSE PARAMETERS WITH $l' = 54.5$ cm AND $R_o = 0.75$

n_i/n_t	Measured			Calculated		
	P (kW)	E (mJ)	t_p (ns)	P (kW)	E (mJ)	t_p (ns)
1.6	22	1	56	45	1.7	37
2.2	110	3	32	140	3.0	21
2.9	440	10	23	270	4.3	16
3.6	400	11	21	450	5.6	13
4.5	630	11	18	680	7.1	10
5.4	640	12	18	920	8.6	9
6.5	710	12	17	1230	10.4	8

Notes:

l' = effective cavity length. P = peak power.
 R_o = output mirror reflectivity. E = peak energy.
 n_i = initial inversion density. t_p = pulse width.
 n_t = threshold inversion density.

Because of the long pulse widths in this system, the peak power and the pulse energy were not measured. As was expected, the pulse widths of this system are all much longer than the range of interest for advanced optical fuzing systems. Figure 8 shows an oscilloscope photograph of the shortest pulse obtained with this system. It exhibits the expected behavior for a Q-switched pulse with a low value of n_i/n_t . It has an almost symmetrical pulse shape as was predicted by Wagner and Lengyel.⁵ The measured values are all slightly longer than the calculated values, but the agreement is good. The limitation on the value of n_i/n_t for low-gain systems makes it impossible to generate a very short pulse in the Q-switched mode. The value of n_i/n_t rarely exceeds 2 for a low-gain system, and even for this value the pulse width would be five times the cavity lifetime. To achieve a value of 2 for n_i/n_t , the mirror reflectivities would have to be high, thereby increasing the cavity lifetime and the subsequent output pulse width.

⁵W. G. Wagner and B. A. Lengyel, *Evolution of the Giant Pulse in a Laser*, *J. Appl. Phys.*, 34 (1963), 2040-2046.

TABLE 5. MEASURED AND CALCULATED Q-SWITCHED PULSE PARAMETERS WITH $\ell' = 74.5$ cm AND $R_o = 0.6$

n_i/n_t	Measured			Calculated		
	P (kW)	E (mJ)	t_p (ns)	P (kW)	E (mJ)	t_p (ns)
1.2	68	4	55	7	0.7	96
1.6	120	5	40	53	2.1	40
2.1	390	12	31	150	3.6	24
2.7	760	17	23	280	4.9	18
3.3	780	18	23	440	6.4	14
4.0	785	18	23	640	8.0	12
4.8	860	19	22	890	9.6	11

Notes:

ℓ' = effective cavity length.
 R_o = output mirror reflectivity.
 n_i = initial inversion density.
 n_t = threshold inversion density.

P = peak power.
E = peak energy.
 t_p = pulse width.

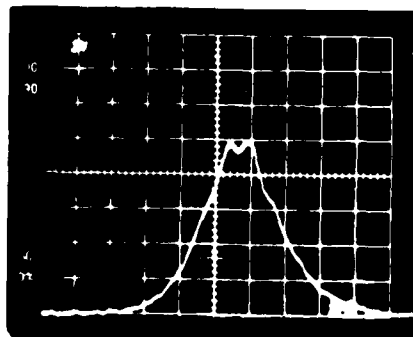


Figure 5. Oscilloscope photograph of shortest Q-switched pulse observed with flashlamp pumped system: cavity length $\ell = 45.7$ cm, output mirror reflectivity $R_o = 0.6$, and initial-to-threshold inversion density $n_i/n_t = 4.8$.

5 ns/DIV



Figure 6. Q-switching setup for continuously pumped Nd:YAG laser rod: output mirror (M1), rear mirror (M2), Nd:YAG rod, horizontal polarizer (P), quarter-wave Pockels cell (PC), and pulse monitor or power meter (PM).

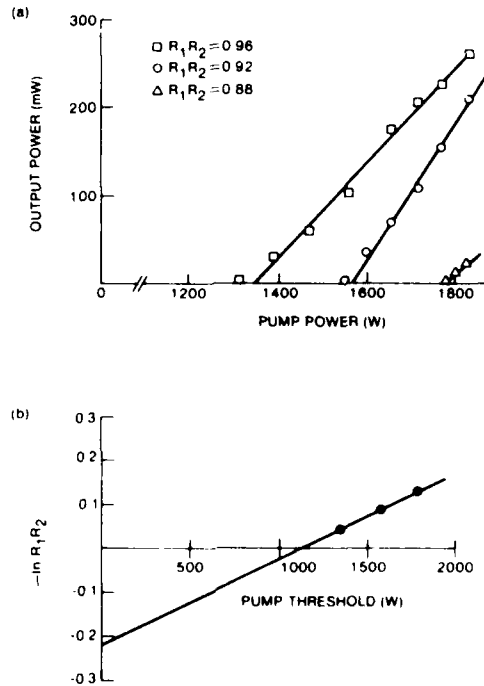


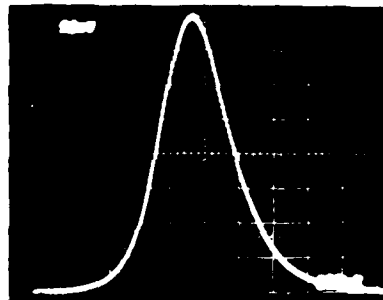
Figure 7. Laser output parameters versus input pump power to determine laser threshold and combined losses for continuously pumped system: (a) continuous wave output power versus pump power to determine threshold for three sets of mirrors and (b) output mirror reflectivity $-\ln R_1 R_2$ versus pump threshold to determine combined losses L .

TABLE 6. CALCULATED Q-SWITCHED PULSE WIDTHS FOR CONTINUOUSLY PUMPED LASER

$R_1 R_2$	n_i/n_t	n_f/n_i	t_c (ns)	t_p (ns)	
				Measured	Calculated
0.96	1.35	0.55	15	230	180
0.92	1.16	0.77	13	380	286
0.88	1.026	0.97	11.3	2000	1050

Notes:

$R_1 R_2$ = output mirror reflectivities. n_f = final inversion density.
 n_i = initial inversion density. t_c = cavity decay time.
 n_t = threshold inversion density. t_p = pulse width.



100 ns/DIV

Figure 8. Oscilloscope photograph of shortest Q-switched pulse obtained with continuously pumped system.

3. CAVITY DUMPING

3.1 Theory

The modulation technique known as cavity dumping is used to generate very short pulses in a slightly different manner than Q-switching. With this technique, the energy is stored in the photon field instead of the population inversion as it is in Q-switching; that is, the Q of the cavity is kept at its maximum value during the pumping cycle. It is maximized by using 100-percent mirrors, which keep the cavity loss at a minimum. When the photon density has built up to its maximum level, the photons are dumped from the cavity by use of an optical switch. Two methods for doing this are shown in figure 9.

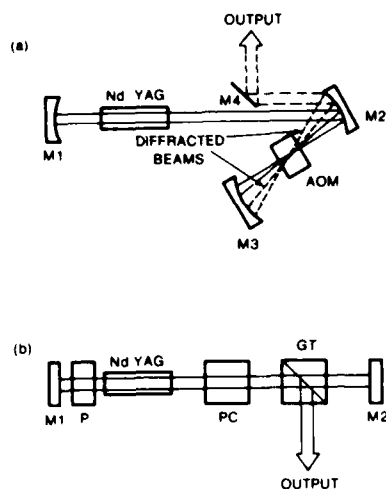


Figure 9. Block diagrams of two cavity dumping techniques: (a) acousto-optic modulator (AOM), 100-percent mirrors (M1 to M4), and continuously pumped Nd:YAG rod and (b) half-wave Pockels cell (PC), 100-percent mirrors (M1 and M2), Glan Thompson escape window (GT), and horizontal polarizer (P).

The first method, which was described by Maydan and Chesler,⁷ uses an acousto-optic modulator as the cavity dumping element. With this technique, the light beam is diffracted (indicated by the dashed lines in fig. 9) when radio frequency (rf) power is applied to the modulator. The diffraction is caused by the interaction of the acoustic waves in the modulator with the light beam. The acoustic wave modulates the index of refraction of the crystal and creates a phase grating that diffracts the beam. When the rf is off, there is no diffraction and the photon field builds up to its maximum. Since the rod is being pumped continuously, the only restriction in repetition rate is caused by the modulator. Repetition rates up to 10 MHz can easily be obtained with this method.¹

The pulse width is determined by the rise time of the modulator and the effective cavity lifetime. Since an acousto-optic modulator deflects only a portion of the primary beam per pass, the effective cavity lifetime can be calculated by assuming that the modulator is a mirror with a certain transmission coefficient. Typical dumping efficiencies of up to 40 percent per pass can be obtained.⁸ Kruegle and Klein⁹ have made an extensive experimental evaluation of this method

¹W. Koechner, *Solid State Laser Engineering*, Springer-Verlag New York, Inc., New York (1976), 444.

⁷D. Maydan and R. B. Chesler, *Q-Switching and Cavity Dumping of Nd:YAG Lasers*, *J. Appl. Phys.*, **42** (1971), 1031-1034.

⁸A. Yariv, *Quantum Electronics*, John Wiley & Sons, Inc., New York (1975), 364.

⁹H. A. Kruegle and L. Klein, *High Peak Power Output, High PRF by Cavity Dumping a Nd:YAG Laser*, *Appl. Opt.*, **15** (1976), 466-471.

using a 10-W cw Nd:YAG laser. They were able to generate 500-W pulses with pulse widths of 25 ns at repetition rates from 200 kHz to 2 MHz. For repetition rates below 200 kHz, the output pulse amplitude becomes unstable. The point where instability begins depends on two distinct parameters. If the rf pulse is long enough to allow the photon field to decay to less than one photon, the buildup of the field becomes erratic because it now depends on the spontaneous emission process, which is random. Also, if the interpulse period is longer than the characteristic photon field oscillation, the field can decay before the dumping pulse, producing random output pulse amplitude. Chesler and Maydan¹⁰ had predicted this behavior and observed it in their experiments. In their experiments, the lower limit on stability was about 100 kHz. The exact value depends on the cavity configuration, the dumping mechanism, and the pumping rate of the laser. They have shown that in the region of stable operation the average power of cavity dumping can nearly equal the cw output power. They calculated that a 1-W laser could produce 50-ns pulses with peak powers of 200 W. There is no fundamental reason that would prohibit the design of this type of system producing 200-W pulses with widths of 10 to 20 ns.

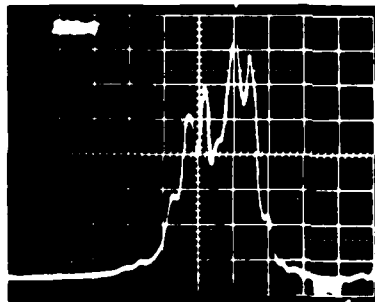
A second method for cavity dumping, shown schematically in figure 9, uses a Pockels cell for dumping the cavity. With this system, horizontally polarized radiation builds up in the cavity during the pumping cycle while the Pockels cell is turned off. When high voltage is applied to the Pockels cell, the polarization is rotated by 90 deg, and the radiation is ejected from the cavity by the Glan Thompson escape window. This dumping technique changes the cavity Q from a very high level to zero in about 10 ns. This means that the cavity is completely dumped in one round-trip time plus the 10-ns turn-on time. Improved Pockels cell electronics could reduce the 10-ns turn-on time and reduce pulse widths to 10 ns or less.

However, the high repetition rates required for stable operation put stringent demands on the Pockels cell pulser. Present Pockels cells require 5 to 10 kV, which would have to be switched at repetition rates of 100 kHz or more. The required operating voltage could probably be reduced by redesign of the Pockels cell to simplify the electronics. With these modifications, a Pockels cell cavity dump laser may provide a source of narrow high peak power pulses for optical fuze applications.

¹⁰R. B. Chesler and D. Maydan, *Calculation of Nd:YAG Cavity Dumping*, *J. Appl. Phys.*, 42 (1971), 1028-1030.

3.2 Experimental Results

Cavity dumping experiments were performed by using the pulsed Nd:YAG laser (sect. 2) with the configuration of figure 9(b). Due to the losses introduced by the cavity dumping elements, we could not make similar measurements with the cw Nd:YAG laser. The pulsed laser produced a pulse with a 10-ns half width and a peak power of 28 kW. The output pulse amplitude was quite variable because, with a pulsed pump, the photon field must build up from zero on each pulse. The spontaneous emission process is quite noisy, so the output pulse amplitude was variable. However, the pulse width depends only on the Pockels cell switching time and the cavity round-trip time. The pulse rise time should follow the Pockels cell rise time, and the fall time should be equal to one round-trip time. For these experiments, the switching time was about 10 ns and the cavity round-trip time was 4 ns. Figure 10 shows an oscilloscope trace of the pulse obtained with this system. The pulse exhibits the characteristic mode beating that has been observed in Q-switched pulses within the cavity dumped envelope. The envelope rise time is about 10 ns and the fall time is about 5 ns, as expected. These agree quite well with the theory.



5 ns/DIV

Figure 10. Oscilloscope photograph of cavity dumped pulse observed by using setup of figure 9(b) and flashlamp pumped Nd:YAG rod.

4. Q-SWITCHED CAVITY DUMPING

4.1 Theory

Pulse modulation by the Q-switched cavity dumping technique, also called PTM mode or double Q-switching, combines the advantages of the Q-switched mode of operation and the cavity dumping technique. Normally, the fall time of a Q-switched pulse is determined by the cavity decay time, and the rise time is determined by the initial inversion level compared with the threshold inversion. By introducing the cavity dumping elements, the fall time of the pulse can be reduced to the round-trip time of the cavity instead of the cavity decay time, which can be quite long.

To see how this technique can be of value, one must refer to section 2. By examining equation (3) for the Q-switched pulse width, it is seen that t_p is always greater than t_c . For high inversion levels, the fall time of the pulse is given by t_c and the rise time of the pulse becomes very short. Cavity dumping the Q-switched pulse essentially reduces the fall time from t_c to t_R , the cavity round-trip time. Hence, t_c can be increased by maximizing the mirror reflectivities without lengthening the pulse. Increasing t_c also lowers the threshold and thereby increases the value of n_i/n_t . This increase allows the minimum possible rise time along with the shortest possible fall time.

The implementation of this technique involves setting up the cavity with all the Q-switching and cavity dumping elements in place using 100-percent mirrors. When the cavity Q is switched to its high value, the Q is at absolute maximum because of the high mirror reflectivity. The threshold is then at its lowest value, increasing the value of n_i/n_t . The pulse rise time is at its minimum value. If the cavity dumping is instantaneous and occurs at the point where the peak power of the Q-switched pulse is obtained, the fall time is limited to t_R with the effect that the peak power output increases. In practice, this increase does not occur since the response time of the cavity dumping element is not instantaneous, and the ideal pulse shape is not obtained.

A computer solution of the laser rate equations for a three-level system operating in this mode has been given by Weidler, Burkholter, and Vuylsteke.¹¹ Their results were applied to a ruby laser system. Their key result showed that as long as the cavity dump switching time is less than one round-trip time, the pulse is triangular with a pulse width equal to one round-trip time of the cavity. The peak power is then increased over the normal Q-switched pulse by a factor of three to five times. This increase was experimentally verified by Rundle.¹² He was able to generate a 5.3-ns pulse with almost symmetric rise and fall times using a switch with a 5-ns rise time. These experiments were duplicated by Ernest, Michon, and Debrie.¹³ Using a 2-ns switching time, they produced pulse widths of 3.5 to 7 ns, depending on the cavity length.

¹¹R. C. Weidler, J. H. Burkholter, and A. A. Vuylsteke, *Computer Solutions of Laser Rate Equations for PTM Q-Switching and Comparison with PRM Results*, *J. Appl. Phys.*, 38 (1967), 4510-4512.

¹²W. J. Rundle, *A Ruby Laser Modified for Pulse-Transmission Mode Cavity Dumping*, *J. Appl. Phys.*, 39 (1968), 5538-5539.

¹³J. Ernest, M. Michon, and J. Debrie, *Giant Optical Pulse Shortening Through Pulse-Transmission Mode Operation of a Ruby Laser*, *Phys. Lett.*, 22 (1966), 147-149.

4.2 Experimental Results

The experiments with this technique were confined to the flash-lamp pumped Nd:YAG laser. It was not feasible to use the cw laser for these experiments, although it would have been a preferred option. The experimental setup is shown in figure 11. With this setup, the double Q-switching occurs as follows. When pumping begins, a quarter-wave voltage is applied to the quarter-wave Pockels cell. This quarter-wave rotation in combination with the quarter-wave plate rotates the polarization 180 deg after reflecting from the mirror and passing back through both elements. At the same time, the Q of the cavity is kept low because, with no voltage applied to the half-wave Pockels cell, the vertical polarizer and the vertical escape window act as crossed polarizers. When the inversion has reached its maximum, a half-wave voltage is applied to the half-wave Pockels cell, and the subsequent 90-deg rotation causes the Q-switching to begin. Once the pulse has reached its maximum level, the quarter-wave voltage is removed from the second Pockels cell with the effect that the polarization is now rotated 90 deg after passing through the quarter-wave plate twice. The radiation is then ejected from the cavity by the escape window.

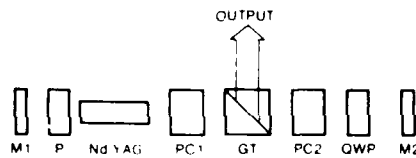


Figure 11. Double Q-switching setup using two kinds of Pockels cells: 100-percent mirror (M1), 75-percent mirror (M2), vertical polarizer (P), Nd:YAG rod, half-wave Pockels cell (PC1), quarter-wave Pockels cell (PC2), Glan Thompson escape window (GT), and quarter-wave plate (QWP).

A typical double Q-switched pulse obtained with the setup of figure 11 is shown in figure 12. Also shown is the Q-switched pulse observed through the 75-percent mirror. For this experiment, the switching time was 10 ns compared with a round-trip time of 5 ns, so the output pulse shape and width were modified only slightly. The rise times of both pulses are approximately the same, but the fall time of the double Q-switched pulse is somewhat less than that of the Q-switched pulse. In fact, the pulse widths are 18 and 21 ns for the double Q-switched and Q-switched pulses, respectively. The same type of pulse widths that have been observed with ruby oscillators^{12,13} could be produced also with the Nd:YAG laser, but the limitation on the repetition rate of flashlamp pumped systems still applies. For these limited experiments, the observed pulse did not approach that which could be produced with fast switching elements, but the agreement with theory is good.

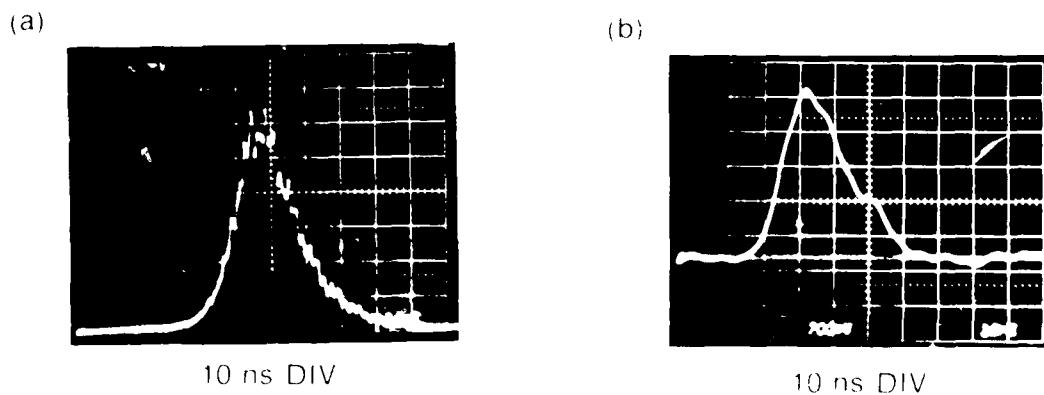


Figure 12. Oscilloscope photographs of (a) double Q-switched pulse observed with 1-ns response detector and (b) Q-switched pulse observed through 75-percent mirror using 4-ns response detector.

¹²W. J. Rundle, A Ruby Laser Modified for Pulse-Transmission Mode Cavity Dumping, *J. Appl. Phys.*, 39 (1968), 5538-5539.

¹³. Ernest, M. Michon, and J. Debrie, Giant Optical Pulse Shortening Through Pulse-Transmission Mode Operation of a Ruby Laser, *Phys. Lett.*, 22 (1966), 147-149.

5. MODE LOCKING

The mode locking technique is used to generate very short pulses at very high repetition rates. A full theoretical treatment of this technique^{8,14,15} is beyond the scope of this report. This technique is generally applied to inhomogeneously broadened laser systems, but it can be applied also to homogeneously broadened lasers. Since Nd:YAG is an inhomogeneously broadened laser crystal, the discussion is limited to the inhomogeneously broadened laser.

In an inhomogeneously broadened material such as Nd:YAG, the laser gain line width is determined by the summation of many individually distinguishable emitters all emitting at slightly different frequencies. Thus, in an Nd:YAG laser, more than one mode can propagate for pumping levels greater than threshold. The situation that exists for this type of laser above threshold is depicted in figure 13. Figure 13(a) shows the gain profile of the laser along with the loss line. The possible cavity modes are indicated, and for this case seven modes have gains that exceed the loss line. Figure 13(b) shows the relative intensities that would be observed with the gain curve shown in figure 13(a). When the phases of these modes are random, the output intensity of the laser exhibits random fluctuations. In mode locking, these phases are locked together so that the output power of the laser is proportional to⁸

$$P(t) \propto \frac{\sin^2\left(\frac{N\omega t}{2}\right)}{\sin^2\left(\frac{\omega t}{2}\right)}$$

⁸A. Yariv, *Quantum Electronics*, John Wiley & Sons, Inc., New York (1975), 256-272.

¹⁴A. Yariv, *Internal Modulation in Multimode Laser Oscillators*, *J. Appl. Phys.*, 36 (1965), 388.

¹⁵M. DiDomenico, *Small Signal Analysis of Internal Modulation of Lasers*, *J. Appl. Phys.*, 35 (1964), 2870.

where N is the number of oscillating modes and ω is the mode spacing given by $\pi c/l'$. It has been assumed also that the intensities of each mode are equal. The output of the laser then has the following characteristics: there is a periodic train of pulses spaced in time by $T = 2l'/c$ with pulse width $\tau = 1/\Delta\nu$, where $\Delta\nu$ is the gain line width. Also, the peak power is N times the average power of the laser. The average power of the laser is unchanged, except that the output is now a train of narrow pulses.

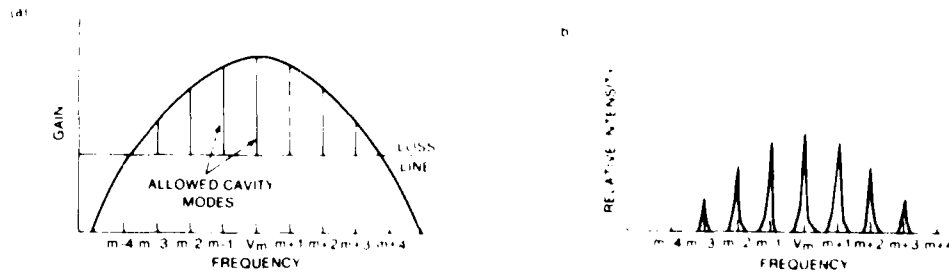


Figure 13. Cavity mode characteristics of inhomogeneously broadened laser: (a) inhomogeneously broadened gain curve showing allowed cavity modes and resonator loss line and (b) relative intensity of allowed oscillating modes above threshold.

Mode locking can be accomplished in a variety of ways. The most common of these is loss modulation. In the loss modulation technique, a setup similar to that in figure 14 is used. The cavity loss is modulated by an acousto-optic modulator, which diffracts some of the energy out of the cavity at specific times. The reflections of the acoustic wave from the opposite side of the modulator create a standing wave pattern at twice the modulation frequency. By adjusting the modulation frequency to exactly one-half the cavity mode spacing, the loss is a minimum, and therefore the gain is a maximum only at certain times. This adjustment forces the oscillation to build up at these times, thereby locking the phases together via the loss modulation. The phases also are restored on each pass so that any mode drifting is eliminated.

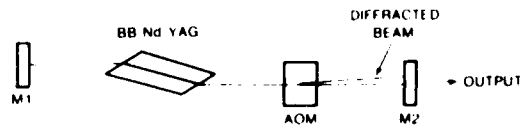


Figure 14. Typical mode locking setup using mirrors (M1 and M2), Brewster-Brewster (BB) Nd:YAG rod, and acousto-optic modulator (AOM).

In this technique, the parameters of prime interest are $\Delta\nu$, the laser gain line width, and the cavity length. For Nd:YAG, $\Delta\nu = 1.2 \times 10^{10}$ Hz; with $l' = 0.5$ m, the mode spacing is 300 MHz. Approximately 40 modes can be locked in this laser if the gain is high enough. The calculated pulse width is 83 ps, compared with a measured value¹⁶ of 76 ps. The peak power is approximately 40 W for a 1-W cw laser.

For optical fuze system applications, this technique poses several problems. First, for a cavity length of 0.5 m, the modulation frequency is 150 MHz and the pulse repetition rate is 300 MHz. The output pulse separation is then 3.3 ns. A compact modulator capable of producing enough rf power to drive an acoustic transducer at these frequencies is difficult to build. Second, the electronics necessary for a target discrimination technique that analyzes pulse return shape to discriminate against clouds, smoke, or dust on a pulse-to-pulse basis is complicated because of the very high repetition rate. The detector also limits the usefulness of this type of discrimination technique because the best detectors available at present can barely follow the rise time of the pulse, and most detectors drastically distort the fall time. The only electronics that are practical can integrate many pulses and use a threshold detection system for decision making. The high repetition rate is an advantage for this type of detection, but it is not clear that a mode locked laser would be needed if this technique were to be used.

¹⁶M. DiDomenico, J. E. Geusic, H. M. Marcos, and R. G. Smith, *Generation of Ultrashort Optical Pulses by Mode Locking the YAG:Nd Laser*, *Appl. Phys. Lett.*, 8, No. 7 (1966), 180.

An alternative to the mode locking technique is a mode locked cavity dumped system. The peak power is increased by using 100-percent mirrors, and the repetition rate is variable. However, the overall efficiency is reduced because the average power is somewhat lower. For this type of system to operate well with cavity lengths of less than 0.5 m, the switching element response time has to be less than 2 ns. The switching has to be synchronized with the mode locked pulse for optimum operation. Detection of the mode locked pulse and subsequent triggering of the switching element have to take place in less than 2 ns since state-of-the-art electro-optic switches have rise times of approximately 1 ns. The electronics required to detect the mode locked pulse and to generate the high voltage pulse required to switch the electro-optic element is difficult or impossible to construct in the limited space available in optical fuze systems.

6. SYSTEM CONSIDERATIONS

To determine the applicability of a particular optical source for use in an optical proximity fuze system, the performance requirements must be met, and the size, the weight, and the cost must be compatible with the system constraints. The general performance requirements addressed here as a baseline are for a source that has better than 100-W peak power, a repetition rate of 1 kHz or better, and pulse widths of 10 ns or less. The size, the weight, and the cost of the source depend on how much the source is required to exceed the baseline requirements, but an estimate at least can be made of the minimum expected for a baseline source. This allows a determination of the type of air-defense or ballistic missile application to be considered.

Reviewing the various modulation techniques that were investigated, some definite conclusions can be made about some of them. First, the flashlamp pumped system can be eliminated because the maximum repetition rate has a practical limit in the 10- to 100-Hz range. Second, the Q-switched and double Q-switched continuously pumped systems can be discarded. These configurations cannot generate sufficiently narrow pulses in the Q-switched mode because of insufficient gain. The continuously pumped minimum pulse width observed with the system used for these experiments was about 200 ns. A higher gain system reduces the pulse width somewhat, but a 10-ns pulse is not feasible. The remaining systems are the mode locked and cavity dumped configurations with continuous pumping. As stated in section 5, the repetition rate of a mode locked system necessarily is very high. It is not clear that there is much benefit in having pulse repetition rates of 100-MHz or greater, and the very narrow pulse width can be an advantage or a disadvantage, depending on the specific system considerations. Since the peak power output of this system is considerably lower than that of the continuously pumped cavity dumped system, the cavity dumping technique is the most promising of the systems.

As discussed in section 2, the cavity dumping technique, when used with a continuously pumped rod, is quite efficient in terms of the average power generated with cavity dumping compared with the cw power. This technique has produced 500-W pulses at repetition rates of 1 MHz and pulse widths of 25 ns from a 10-W laser. With some modifications in the cavity dumping technique, pulse widths of 10 ns can be achieved. There are some serious drawbacks to this type of laser system, however; to generate 1 W of single mode cw power, 1 kW of electrical power is required continuously.

The efficiency of high power multimode cw lasers can approach 1 percent in similar configurations, but these lasers require 10 kW of input power to generate 50 to 100 W of cw power. Because of the low efficiency of cw lasers, a large cooling capacity also is required. The efficiency of these lasers can be improved by pumping harder, improving the pumping efficiency, and maximizing the output with respect to mirror transmission. Considering the power restrictions, improving the pumping efficiency is the most useful method for optical fuzing systems. Reno and Herzog¹⁷ have demonstrated just such a system. They improved the pumping efficiency by replacing the conventional lamps in an Nd:YAG laser with multiple arrays of gallium aluminum arsenide (GaAlAs) laser diodes. These diodes are wavelength tuned so that they pump directly into the absorption bands of the Nd:YAG crystal. Almost all the output power of the diodes is then absorbed by the laser rod. Reno and Herzog were able to generate 125 mW of single mode cw power with a pump input power of 50 W. The efficiency at this pumping level, which is near threshold, is only 0.2 percent compared with a typical efficiency of 0.1 percent for cw Nd:YAG lasers above threshold. This efficiency can be increased markedly by increasing the pumping level.

To get an idea of the improvement that could be expected by doubling the pumping power, consider the cw Nd:YAG laser used in our experiments. At an 1800-W input, our laser produced 1 W, but at a 1200-W input, it produced only 0.15 W. This decrease corresponds to an increase of four times in efficiency for a 50-percent increase in pumping power. This efficiency would imply that doubling the pumping power would increase the output power by at least eight times. It would then be reasonable to expect that a system similar to the one built by Reno and Herzog would produce 1 W for a pumping power of 100 W. The compactness of this approach would make it ideal for optical fuze systems. However, there is one serious drawback--the cost. A considerable amount of research and development would be required to produce the pumping diodes, and the system would have to be built and demonstrated. It is therefore difficult to estimate the actual cost for this technique.

¹⁷C. W. Reno and D. G. Herzog, *Diode Pumped Nd:YAG Laser Development*, RCA, Camden, NJ, Report ATL-CR-76-02 (May 1976).

7. SUMMARY

Four techniques for modulating an Nd:YAG laser have been evaluated from an optical fuzing standpoint: Q-switching, cavity dumping, double Q-switching, and mode locking. The theory is compared with experimental results for the first three methods, and the agreement is good. For the mode locking technique, the discussion is limited to a general description of the technique. It was determined from our results that the only system that met the system requirements or could be modified to do so is the cavity dumping technique using a continuously pumped rod. The power and cooling requirements of the lamps used for pumping limit the usefulness of this system. A diode pumped system operating in the cavity dump mode is the most practical because of its high efficiency, perhaps approaching 1 percent. To determine the practicability of this system, however, a considerable amount of research and development is required. In short, a continuously pumped cavity dumped system can meet the system requirements, but an analysis of the power, cooling, and space requirements of the source with respect to availability in the fuze system is necessary.

LITERATURE CITED

- (1) W. Koechner, Solid State Laser Engineering, Springer-Verlag New York, Inc., New York (1976).
- (2) R. W. Hellwarth, Advances in Quantum Electronics, Columbia University Press, New York (1961), 334-341.
- (3) E. J. McClung and R. W. Hellwarth, Characteristics of Giant Optical Pulsations from Ruby, Proc. IEEE, 51 (1963), 46-53.
- (4) A. A. Wylsteke, Theory of Laser Regeneration Switching, J. Appl. Phys., 34 (1963), 1619-1622.
- (5) A. A. Wylsteke and R. A. Develoy, Evolution of the Giant Pulse in a Laser, J. Appl. Phys., 34 (1963), 2040-2046.
- (6) R. W. Hellwarth, Optics, Holt, Rinehart & Winston, Inc., New York (1962), 277-282.
- (7) A. A. Wylsteke, Theory of Regeneration and Cavity Dumping of Lasers, J. Appl. Phys., 34 (1963), 1331-1334.
- (8) R. W. Hellwarth, Optics, Holt, Rinehart & Winston, Inc., New York (1962), 277-282.
- (9) R. W. Hellwarth, High Power Output, High PRF by Regeneration Switching, J. Appl. Phys., 35 (1964), 466-471.
- (10) A. A. Wylsteke, Theory of Q-Switching and QWYAG Cavity Dumping, J. Appl. Phys., 35 (1964), 2611-2614.
- (11) A. A. Wylsteke, R. A. Develoy, and A. A. Wylsteke, Computer Simulation of Regeneration Switching, PDM, Q-Switching and Cavity Dumping, J. Appl. Phys., 38 (1967), 4510-4512.
- (12) R. W. Hellwarth, A Simple Method for Pulse-Transmission Mode Operation of Lasers, J. Appl. Phys., 34 (1963), 5538-5539.
- (13) R. W. Hellwarth, M. M. Perlman, and J. Sobrie, Giant Optical Pulse Short-Duration Regeneration Switching Mode Operation of a Ruby Laser, Optics Letters, 1 (1967), 142-143.
- (14) A. Yariv, Internal Modulation in Multimode Laser Oscillators, J. Appl. Phys., 36 (1965), 388.
- (15) M. Imboden, Small Signal Analysis of Internal Modulation of Lasers, J. Appl. Phys., 35 (1964), 2870.

LITERATURE CITED (Cont'd)

- (16) M. DiDomenico, J. E. Geusic, H. M. Marcos, and R. G. Smith, Generation of Ultrashort Optical Pulses by Mode Locking the YAlG:Nd Laser, *Appl. Phys. Lett.*, 8, No. 7 (1966), 180.
- (17) C. W. Reno and D. G. Herzog, Diode Pumped Nd:YAG Laser Development, RCA, Camden, NJ, Report ATL-CR-76-02 (May 1976).

DISTRIBUTION

COMMANDER
 US ARMY COMMUNICATIONS RESEARCH AND
 DEVELOPMENT COMMAND
 ATTN DRDCO-PT, PRODUCT ASSURANCE
 & TEST DIR
 ATTN DRDCO-PE, PRODUCTION ENGR
 SUPPORT DIR
 FT. MONMOUTH, NJ 07703

COMMANDER
 US ARMY COMMUNICATIONS & ELECTRONICS
 MATERIEL READINESS COMMAND
 ATTN SELEM-QA, QUALITY ASSURANCE OFC
 FT. MONMOUTH, NJ 07703

DIRECTOR
 ELECTRONIC WARFARE LABORATORY
 ATTN DELEW-PE, PRODUCTION ENGR OFC
 FT. MONMOUTH, NJ 07703

COMMANDER
 US ARMY FOREIGN SCIENCE
 & TECHNOLOGY CENTER
 ATTN DRXST-IS3, LIBRARY
 FEDERAL OFFICE BLDG
 220 7TH STREET, NE
 CHARLOTTESVILLE, VA 22901

COMMANDER
 US ARMY MATERIALS & MECHANICS
 RESEARCH CENTER
 ATTN DRXMR-PL, TECHNICAL LIBRARY
 ATTN DRXMR-T, MECHANICS RES LAB
 ATTN DRXMR-X, DR. F. S. WRIGHT
 ATTN DRXMR-MI, GEORGE A DARCY
 WATERTOWN, MA 02172

COMMANDER
 US ARMY MISSILE MATERIEL
 READINESS COMMAND
 ATTN DRSMI-Q, DIR FOR PRODUCT
 ASSURANCE
 REDSTONE ARSENAL, AL 35809

COMMANDER
 US ARMY MISSILE RES & DEV COMMAND
 ATTN DRDMI-ET, TEST & EVALUATION DIR
 ATTN DRDMI-Q, PRODUCT ASSURANCE DIR
 ATTN DRDMI-E, HORACE LOWERS
 REDSTONE ARSENAL, AL 35809

COMMANDER
 US ARMY NATICK RES & DEV COMMAND
 US ARMY NATICK DEVELOPMENT CENTER
 ATTN DRDNA-T, TECHNICAL LIBRARY
 NATICK, MA 01760

DIRECTOR
 NIGHT VISION & ELECTRO-OPTICS LAB
 ATTN DELNV-L LASER DIV
 FORT BELVOIR, VA 22060

DIRECTOR
 US ARMY RESEARCH AND TECHNOLOGY
 LABORATORIES
 AMES RESEARCH CENTER
 ATTN SAUDL-AS, FRED IMMEN
 MOFFETT FIELD, CA 94035

DIRECTOR
 US ARMY SIGNALS WARFARE LABORATORY
 ATTN DELSW-TE, TEST & EVAL OFC
 VINT HILL FARMS STATION
 WARRENTON, VA 22186

COMMANDER
 US ARMY TANK-AUTOMOTIVE MATERIEL
 READINESS COMMAND
 DEPT OF THE ARMY
 ATTN DRSTA-F,
 DIR FOR MATERIEL MANAGEMENT
 WARREN, MI 48090

COMMANDER
 US ARMY TANK-AUTOMOTIVE RES
 & DEV COMMAND
 DEPT OF THE ARMY
 ATTN DRCPM-CVT, ARMORED COMBAT
 VEHICLE TECHNOLOGY
 WARREN, MI 48090

COMMANDER
 HQ, US ARMY TEST & EVALUATION COMMAND
 ATTN DRSTE-CT, COMBAT SUPPORT SYS
 MATERIEL TEST DIR
 ABERDEEN PROVING GROUND, MD 21005

COMMANDER
 WHITE SANDS MISSILE RANGE
 DEPT OF THE ARMY
 ATTN STEWS-TE, ARMY MAT TEST
 & EVALUATION DIR
 WHITE SANDS MISSILE RANGE, NM 88002

COMMANDER
 EDGEWOOD ARSENAL
 ATTN SAREA-TS, TECH LIB
 EDGEWOOD ARSENAL, MD 21010

COMMANDER
 ROCK ISLAND ARSENAL
 ATTN SARRI-ENE, ENGR & TEST DIV
 ROCK ISLAND, IL 61201

COMMANDER
 US ARMY ABERDEEN PROVING GROUND
 ATTN STEAP-TL, TECH LIB
 ABERDEEN PROVING GROUND, MD 21005

COMMANDER
 US ARMY ELECTRONICS PROVING GROUND
 ATTN STEEP-PA-I, TECH INFO CENTER
 FORT HUACHUCA, AZ 85613

DISTRIBUTION (Cont'd)

ADMINISTRATOR
DEFENSE DOCUMENTATION CENTER
ATTN DDC-TCA (12 COPIES)
CAMERON STATION, BUILDING 5
ALEXANDRIA, VA 22314

COMMANDER
US ARMY RSCH & STD GP (EUR)
ATTN CHIEF, PHYSICS & MATH BRANCH
FPO NEW YORK 09510

COMMANDER
US ARMY ARMAMENT MATERIEL
READINESS COMMAND
ATTN DR SAR-LFP-L, TECHNICAL LIBRARY
ATTN DR SAR-ASF, FIRE & MUN
SUPPORT DIV
BARK ISLAND, IL 61299

COMMANDER
US ARMY MISSILE & MUNITIONS
CENTER & SCHOOL
ATTN ATSK-CTD-F
REDSTONE ARSENAL, AL 35809

DIRECTOR
US ARMY MATERIEL SYSTEMS
ANALYSIS ACTIVITY
ATTN DEXSY-MP
ABERDEEN PROVING GROUND, MD 21005

DIRECTOR
US ARMY BALLISTIC RESEARCH LABORATORY
ATTN DR DAR-TSB-F (STEIN)
ABERDEEN PROVING GROUND, MD 21005

USAF SAMI
WASHINGTON, DC 20330

TELEPHONE BROWN ENGINEERING
COMMUNIC RESEARCH PARK
ATTN DR. MELVIN L. PRICE, MS-44
HUNTSVILLE, AL 35807

ENGINEERING SOCIETIES LIBRARY
41 EAST 47TH STREET
ATTN ACQUISITIONS DEPARTMENT
NEW YORK, NY 10017

US ARMY ELECTRONIC TECHNOLOGY
& DEVELOPMENT LABORATORY
ATTN DELET-ED
FORT MONMOUTH, NJ 07703

BROOKHAVEN NATIONAL LABORATORY
ASSOCIATED UNIVERSITIES, INC.
ATTN MECHANICAL ENGINEERING
ATTN PHYSICS DEPT
UPTON, LONG ISLAND, NY 11973

DEPARTMENT OF COMMERCE
NATIONAL BUREAU OF STANDARDS
ATTN LIBRARY
ATTN GEORGE BIRNBAUM
WASHINGTON, DC 20234

DIRECTOR
DEFENSE COMMUNICATIONS AGENCY
ATTN TECH LIBRARY
WASHINGTON, DC 20305

DIRECTOR
DEFENSE COMMUNICATIONS
ENGINEERING CENTER
ATTN TECHNICAL LIBRARY
1860 WIEHLE AVE
RESTON, VA 22090

DIRECTOR
DEFENSE NUCLEAR AGENCY
ATTN STSP, SHOCK PHYSICS DIRECTORATE
WASHINGTON, DC 20305

UNDER SECRETARY OF DEFENSE
FOR RESEARCH & ENGINEERING
ATTN DEP DIR (TEST & EVALUATION)
WASHINGTON, DC 20301

OFFICE OF THE DEPUTY CHIEF OF STAFF
FOR RESEARCH, DEVELOPMENT,
& ACQUISITION
ATTN DAMA-ARZ-A, CHIEF SCIENTIST,
DA & DIRECTOR OF ARMY RESEARCH,
DR. M. E. LASSER
ATTN DAMA-CSM, MUNITIONS DIV
DEPARTMENT OF THE ARMY
WASHINGTON, DC 20310

COMMANDER
US ARMY ARMAMENT RESEARCH AND
DEVELOPMENT COMMAND
ATTN DR DAR-SEM, MATERIEL DEV EVAL
ATTN DR DAR-QA, PRODUCT ASSURANCE DIV
ATTN DR DAR-TS, TECHNICAL SUPPORT DIV
ATTN DR DAR-QAR-L, MARK WEINBERG
ATTN DR DAR-LCA, PAUL KISATSKY
ATTN DR DAR-QAN, P. G. OLIVIERI
DOVER, NJ 07801

COMMANDER
ARBCOM
ATTN DR SAR-MAD-C,
AMMUNITION MAINTENANCE ENGR BR
DOVER, NJ 07801

COMMANDER
US ARMY ARMOR CENTER
ATTN TECHNICAL LABORATORY
FORT KNOX, KY 40121

DISTRIBUTION (Cont'd)

COMMANDER
US ARMY YUMA PROVING GROUND
ATTN STEYP-MSA, TECHNICAL LIB
YUMA, AZ 85364

CHIEF OF NAVAL RESEARCH
DEPT OF THE NAVY
ATTN TECHNICAL LIBRARY
ARLINGTON, VA 22217

SUPERINTENDANT
NAVAL POSTGRADUATE SCHOOL
ATTN LIBRARY, CODE 2124
MONTEREY, CA 93940

DIRECTOR
NAVAL RESEARCH LABORATORY
ATTN 2600, TECHNICAL INFO DIV
WASHINGTON, DC 20375

COMMANDER
NAVAL SEA SYSTEMS COMMAND HQ
DEPT OF THE NAVY
ATTN NSEA-09G32, TECH LIB
WASHINGTON, DC 20362

COMMANDER
NAVAL SHIP R&D CENTER
ATTN LIBRARY DIV
BETHESDA, MD 20834

COMMANDER
NAVAL SURFACE WEAPONS CENTER
ATTN DX-21, LIBRARY DIV
DAHLGREN, VA 22448

COMMANDER
NAVAL SURFACE WEAPONS CENTER
ATTN WX-40 TECHNICAL LIB
WHITE OAK, MD 20910

COMMANDER
NAVAL WEAPONS CENTER
ATTN 06, TEST & EVALUATION DIV
CHINA LAKE, CA 94555

COMMANDER
HQ AIR FORCE SYSTEMS COMMAND
ANDREWS AFB
ATTN TECHNICAL LIBRARY
WASHINGTON, DC 20334

DEFENSE STATE UNIV. DEPT OF ME
ATTN LAWRENCE CALDER
SUNNYSIDE, ME 04461

GENERAL DYNAMICS
ATTN P. R. DE TONNANCOUR (LIBRARIAN)
P.O. BOX 748
FORT WORTH, TX 76101

BETHLEHEM STEEL CORP
ATTN RICHARD KLINMAN
BUILDING A RM C128
BETHLEHEM, PA 18016

TENN. TECH. UNIVERSITY
ATTN DR. J. RICHARD HOUGHTON
COLLEGE OF ENGINEERING
COOKEVILLE, TN 38501

JOHNS HOPKINS UNIVERSITY
ATTN DR. ROBERT GREEN
MATERIAL SCIENCES & ENGINEERING
BALTIMORE, MD 21218

UNIVERSITY OF HULL
ATTN DR. R. J. DEWHURST
DEPT OF APPL. PHYSICS
HULL, HU6 7EX
ENGLAND

UNIVERSITY OF HOUSTON
ATTN DR. C. GERALD GARDNER
PROF. OF ENG. SCIENCE
CULLEN COLLEGE OF ENG.
HOUSTON, TX 77004

US ARMY ELECTRONICS RESEARCH
& DEVELOPMENT
ATTN TECHNICAL DIRECTOR, DRIEL-CT

HARRY DIAMOND LABORATORIES
ATTN COORDINATOR DIVISION DIRECTORS
ATTN RECORD COPY, 81200
ATTN HDL LIBRARY, 81100 (3 COPIES)
ATTN HDL LIBRARY, 81100 (WOODBRIDGE)
ATTN TECHNICAL REPORTS BRANCH, 81300
ATTN CHAIRMAN, EDITORIAL COMMITTEE
ATTN LEGAL OFFICE, 87000
ATTN J. NEMARICH, 13300
ATTN J. SUTANKAY, 13300
ATTN D. GILBO, 15300
ATTN CHIEF, 13000
ATTN CHIEF, 11000
ATTN CHIEF, 95000
ATTN R. JOHNSON, 15200
ATTN N. KARAYIANIS, 13200
ATTN R. N. SVETTER, 13400
ATTN C. LANHAM, 00213
ATTN W. ISLE, 13500
ATTN S. GRAYBILL, 22400
ATTN R. WELLMAN, 13300 (20 COPIES)

**DATE
FILMED**

— 8